

μ	dipole moment
η	association factor
ω	acentric factor

Subscripts

c	critical constant
exptl	experimental
H	homomorph compound
L	liquid phase
T	temperature
V	vapor phase

Registry No. Me₂CO, 67-64-1; 2-PrOH, 67-63-0; PrOH, 71-23-8.

Literature Cited

- (1) Prausnitz, J. M.; Eckert, C. A.; Orye, R. V.; O'Connell, J. P. *Computer Calculations For Multicomponent Vapor-Liquid Equilibrium*; Prentice-Hall: Englewood Cliffs, NJ, 1967.
- (2) Freshwater, D. C.; Pike, K. A. *J. Chem. Eng. Data* **1987**, *12*, 179.
- (3) Ocan, J.; Tojo, G.; Bao, M.; Arce, A. *An. R. Soc. Esp. Fis. Quim.* **1973**, *69*, 673.
- (4) Gmehling, J.; Onken, U.; Art, W. *Vapor-Liquid Equilibrium Data Collection*; Dechema: Dortmund, 1982; Vol. I, Part 2C, p 487.
- (5) Hipkin, H.; Myers, H. S. *Ind. Eng. Chem.* **1954**, *46*, 2524.

- (6) Gillespi, D. T. C. *Ind. Eng. Chem., Anal. Ed.* **1946**, *18*, 575.
- (7) Nielsen, R. L.; Weber, J. H. *J. Chem. Eng. Data* **1959**, *4*, 145.
- (8) Wagner, I. F.; Weber, J. H. *Chem. Eng. Data Ser.* **1958**, *3*, 220.
- (9) Carnahan, B.; Luther, H. A.; Wilkes, J. O. *Applied Numerical Methods*; Wiley: New York, 1969; Chapter 1.
- (10) Wilson, G. M. *J. Am. Chem. Soc.* **1964**, *86*, 127.
- (11) Gottfried, B. S.; Weisman, J. *Introduction to Optimization Theory*; Prentice-Hall: Englewood Cliffs, NJ, 1973; Chapter 2.
- (12) Herington, E. F. G. *Nature* **1947**, *160*, 610.
- (13) Redlich, O.; Kister, A. T. *Ind. Eng. Chem.* **1948**, *40*, 435.
- (14) Ellis, S. R. M.; Bourne, J. R. *Proceedings of the International Symposium on Distillation, Brighton, England*; Institute of Chemical Engineers: Rugby, U.K., 1960.
- (15) Prausnitz, J. M. *Molecular Thermodynamics of Fluid-Phase Equilibria*; Prentice-Hall: Englewood Cliffs, NJ, 1969; Part 3.
- (16) Holland, C. D. *Fundamentals of Multicomponent Distillation*; McGraw-Hill: New York, 1981; p 511.
- (17) O'Connell, J. P.; Prausnitz, J. M. *Ind. Eng. Chem. Process Des. Dev.* **1987**, *6*, 245.
- (18) Ried, C. R.; Prausnitz, J. M.; Sherwood, T. K. *The Properties of Gases and Liquids*, 3rd Ed.; McGraw-Hill: New York, 1977; Chapter 6.
- (19) Ried, L. *Chem. Ing. Tech.* **1954**, *26*, 83.
- (20) Gütökin, N. *J. Karadeniz Univ. Fac. Arts Sci. Chem. Biol., Trabzon* **1985**, *1*, 25.
- (21) Weast, R. C. *CRC Handbook of Chemistry and Physics*; CRC Press: Cleveland, OH, 1976; Part C-57.

Received for review March 8, 1988. Revised May 3, 1988. Accepted October 27, 1988.

Simple Apparatus for Vapor-Liquid Equilibrium Measurements with Data for the Binary Systems of Carbon Dioxide with *n*-Butane and Isobutane

Lloyd A. Weber

Center for Chemical Engineering, Thermophysics Division, National Institute of Standards and Technology, † Gaithersburg, Maryland 20899

We describe the design, construction, and testing of a simple vapor-liquid equilibrium apparatus designed for measurements in the range 300–500 K at pressures to 150 bar. Data are given for measurements of P , T , x , and y for binary systems of carbon dioxide with *n*-butane and isobutane in the range 310–394 K.

Introduction

This apparatus was designed to fill the need for measurements in the temperature range of 300–500 K, which is important both industrially and theoretically and includes the supercritical region of carbon dioxide. It complements an earlier cryogenic apparatus in our laboratory and is similar in principle to a number of existing devices, with, however, one or two novel differences. It satisfies our criteria for an apparatus that is simple in design, easy to build using mostly commercially available components, and capable of efficient acquisition of accurate data.

In the next section we give details of the design and construction of the apparatus and also estimates and results of tests of the accuracy of the various measured quantities. Following that we present data for the systems CO₂ + *n*-butane and CO₂ + isobutane in the range from 310 to 394 K. These data represent a continuation of our earlier work on these systems (1), where we have made measurements from 250

to 280 K. That earlier work was performed with the cryogenic apparatus.

In this temperature range several studies have previously been made on the CO₂ + *n*-butane system: Besserer and Robinson (2) and Behrens and Sandler (3) at 310.9 K, Poettman and Katz (4), 305–415 K, Olds et al. (5), 311–411 K, and Hsu, Nagarajan, and Robinson (6), 319–378 K. For the system with isobutane Besserer and Robinson (7) measured isotherms in the range 311–394 K. A recent publication by Leu and Robinson (8) gives data for CO₂ with both *n*-butane and isobutane in the range 368–418 K. Some of our data were measured at the same temperatures as these references, and comparisons are made where the isotherms coincide.

Apparatus

The apparatus is shown schematically in Figure 1. It is a vapor and liquid recirculation type. Central to the design is a commercial, top-loading convection oven. The oven is lighted and is equipped with a three-layer glass window for visual observations. In place of the hinged lid, we substituted a lift-off top constructed from 1-in.-thick closed-cell foam, faced with aluminum foil and sandwiched between two layers of 0.5-in. plywood. All of the apparatus is either mounted on top of this lid or suspended from the underside to facilitate adjustments and modifications. The oven temperature is controlled by means of a solid-state device that utilizes a J-type thermocouple for a sensor and has a 4–20-mA output to a proportioning SCR power controller that drives the 3-kW heater. A large fan provides vigorous convection, and we have added some baffles

† Formerly National Bureau of Standards.

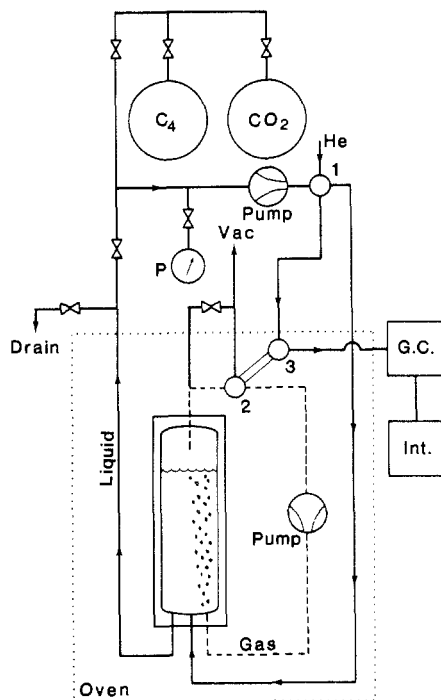


Figure 1. Schematic drawing of the apparatus. See text for explanation.

to improve the mixing in the air bath and reduce thermal gradients. Small, low-power cartridge heaters are mounted on valves 2 and 3 to maintain the vapor sample volume at a temperature slightly warmer than the oven.

The sample cell was developed from a high-pressure sight level gage of a type often used with high-pressure boilers. The body of the cell is a cylindrical cavity (approximately 65 cm³) machined from a bar of 300 series stainless steel. One side of the bar is milled out to accommodate a full-length thick glass window, which is held in place by a very heavy steel flange attached to the body with U-bolts. The ends of the body are drilled and tapped for attaching brass end caps into which are soldered four stainless steel capillary tubes. The caps also have wells for thermometers. The sample cell has a rated maximum pressure of 190 bar at room temperature which decreases to 103 bar at 670 K.

Temperature is measured with a long-stem probe-type platinum thermometer inserted through the top of the oven and into the top cap of the sample cell. It has a nominal resistance of 100 ohms and has a calibration accuracy of 0.025 K. An ac bridge is used for the measurements, and the calibration was checked at one point utilizing a water triple point cell. The bridge can be balanced with a precision of 0.025 K, and the unbalance, in the form of a large dc voltage, is monitored with a digital voltmeter. In normal operation temperature changes of 0.005 K are easily detected.

The vapor recirculating line and pump are mounted entirely within the oven to prevent condensation. A separate liquid-recirculating line takes liquid from the bottom of the cell, out of the oven, through a pump, back into the oven, and into the bottom of the cell. The pressure in the system is measured in this line by means of a gauge outside the oven. In each line there is a rotary sampling valve (1 and 2 in the figure) in which a small sample can be simultaneously trapped and swept out by a carrier gas for analysis. Sample sizes are 1 μ L for the liquid and 20 μ L for the vapor. Valve 3 in the figure selects either vapor or liquid samples. The vapor valve can be evacuated to eliminate the carrier gas between samplings.

The vapor pump is a magnetically driven piston-in-cylinder type with a check valve at each end. The magnet is moved by means of a variable-speed electric motor mounted outside

the oven. The liquid pump is a dual-piston, variable-flow (0–10 cm³/min) model capable of reaching pressures up to 340 bar. It is mounted outside the oven. The pistons are 180° out of phase to minimize pulsations in the line. It is turned off during the pressure measurement. Its main purpose is to circulate the liquid for sampling, but it can also be used to charge the cell with the components from external, room temperature cylinders. Flow rates are kept low to minimize pressure gradients and to allow maximum equilibration time when the liquid reenters the oven.

Pressure is measured with an optically sensed bourdon gauge having a stainless steel helical bourdon tube and digital readout. The pressure in the tube is sensed by the movement of a metal tab which impinges on the path of a light beam, thus eliminating the need for mechanical linkages. The zero and span can be set with mechanical adjustments. Two gauges are used having ranges 0–34 and 0–138 bar. These are small volume gauges and they are connected into the liquid recirculating line with tees. Two sintered steel filters in this line protect the pump and gauges from foreign particles and also serve as pulse dampeners. These gauges have a claimed accuracy of $\pm 0.05\%$ of full scale and were supplied with calibrations. In practice it was found necessary to recalibrate and to check the calibrations periodically. The primary calibration was done by comparison with an oil-operated dead-weight pressure balance, and the subsequent checks were made against a secondary standard steel spiral bourdon gauge having a range of 0–70 bar. We estimate the uncertainty of the pressure measurements to be generally ± 0.03 bar.

The short-term stability of the oven temperature was determined by inserting the thermometer directly into the air bath. It indicated that the air temperature oscillates with a period of about 2 min and an amplitude of about ± 0.03 K. In a heavy metal body such as the sample cell this oscillation is damped to less than ± 0.01 K. Since the controller has no provision for integrating, long-term temperature stability depends somewhat on external conditions, such as changes in room temperature and use of the 50-W oven light. This drift, which might amount to as much as several tenths of a degree from day to day, is compensated manually by means of an external precision variable resistor wired into the circuit of the controller (manual reset). In this way the oven temperature can be set or readjusted to within about 0.01 K. Checks of the homogeneity of the temperature originally showed variations of about 0.1 K before the baffles were added. Afterward the maximum temperature range encountered in the workspace was about 0.05 K. Presumably this could be reduced further by refinements in the baffling.

The vapor compositions, y , and liquid compositions, x , were determined with a gas chromatograph, thermal conductivity bridge, and electronic integrator. The relative response factors of the components, carbon dioxide, *n*-butane, and isobutane in the helium carrier gas were determined with the pure components. Small samples of known relative sizes were used, covering the range encountered experimentally, and the linearity of the results indicated constant response factors for all the components. The integrator has a sensitivity of 0.02 mol %, and the column could easily separate the components.

Samples came from a cylinder of CO₂ having a stated purity of 99.99% and butane cylinders having purities from 99.94% to 99.99%. The only impurity seen on the chromatograph was a small amount (0.02%) of a lighter substance, possibly propane, in the *n*-butane.

Tests of the Apparatus

Other phase equilibrium measurements have been reported in the literature for these systems, and comparisons with those results are made in a later section. Here we are concerned

Table I. Vapor Pressures of the Butanes^a

<i>n</i> -Butane			
<i>T</i>	<i>P</i> _{exptl}	<i>P</i> (9)	<i>P</i> (5)
309.1	3.36	3.39	3.39 ^b
344.26	8.32	8.31	8.31
369.26	14.17	14.14	
394.26	22.52	22.52	
Isobutane			
<i>T</i>	<i>P</i> _{exptl}	<i>P</i> (10)	<i>P</i> (7)
310.93	4.97	5.01	5.03
344.26	11.15	11.13	11.72
369.26	18.48	18.44	
394.26	28.93	28.92	30.20

^a *T* in K and *P* in bar. ^b Adjusted to the temperature of present results.

with more direct tests of the ability of the apparatus to control and measure the experimental quantities of temperature, pressure, and composition. We measured the vapor pressures of the butanes at the temperatures of the four isotherms reported here. The results are shown in Table I. References 9 and 10 are correlations by Goodwin and Haynes of the best available published data for the thermophysical properties of the butanes. We see that the agreement is good and is generally less than the combined estimated uncertainties. We also measured a series of vapor pressures for CO₂ in the region of the critical point at temperatures between 300.35 and 304.07 K. Comparison with the best available published vapor pressures (11) indicates that our pressures are systematically high by 0.07 ± 0.03 bar, or 0.1%. Careful recalibration of the pressure gauges verified this difference. Estimated temperature uncertainties could account for 0.04 bar of this difference. Two measurements were made of the vapor pressure of CClF₃ (R-13) at 298.15 and at 300.25 K. Our values, 35.67 and 37.38 bar, respectively, can be compared with the recent curve published by Fernandez-Fassnacht and del Rio (12). That curve, fitted to their precise data, yields values of 35.65 and 37.38 bar at these temperatures, in excellent agreement with our results.

We also used the apparatus to estimate the critical point of CClF₃. The temperature controller and 3-kW heater are too crude for this purpose. However, since the critical point is quite near room temperature, we were able to control the oven temperature manually with the 50-W light bulb, utilizing very slow heating and cooling curves, and observing the appearance and disappearance of the meniscus. The values we obtained are $T_c = 301.92 \pm 0.04$ K and $P_c = 38.85 \pm 0.04$ bar. The critical parameters of this refrigerant have been measured many times and a comprehensive survey is given by Oguchi et al. (13). Nine of the eleven determinations listed there agree quite well, and a grand average of these yields $T_c = 301.92 \pm 0.03$ K and $P_c = 38.71 \pm 0.20$ bar. We also attempted to estimate the critical parameters of CO₂, but again the temperature control was not adequate for this exacting job. Our best estimate from the disappearance of the meniscus is that T_c is between 304.07 and 304.14 K. The best current determination of T_c for CO₂ is 304.13 K.

Examination of the equilibrium data for dilute solutions of CO₂ (component 1) in butane (component 2) provides further information about the accuracy of the data. Plots of $(P - P_2^\sigma)/x_1$ versus $(P - P_2^\sigma)$, where *P* is the total vapor pressure of the mixture, *P*₂^σ is the vapor pressure of pure 2, and *x*₁ is the mole fraction of 1 in the liquid phase, are a stringent test of the precision and accuracy of the pressure and composition measurements. Theory says that these curves should approach the infinitely dilute solution (pure 2) as horizontal straight lines. Plots of our data indicate this behavior and the precision of the data are consistent with statistical uncertainties of ± 0.03 bar in

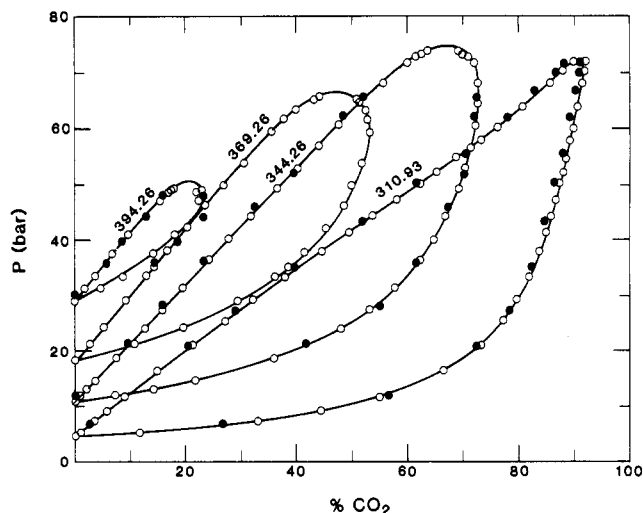


Figure 2. Phase compositions for the system CO₂ + isobutane. Filled circles are from ref 7.

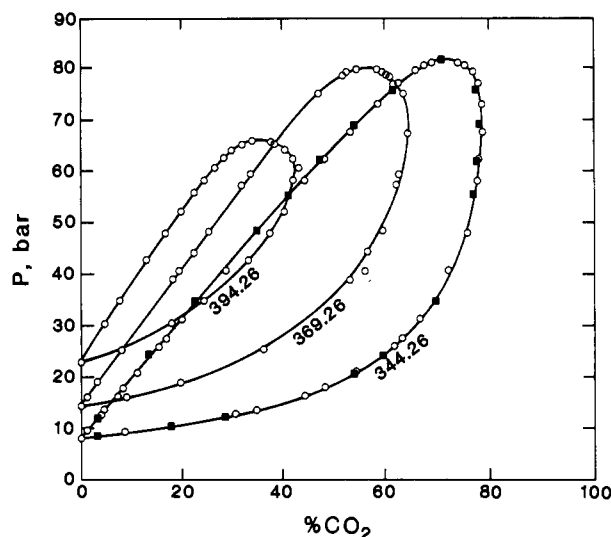


Figure 3. Phase compositions for the system CO₂ + *n*-butane. Filled squares are from ref 5.

pressure and/or ± 0.03 mol % in composition.

From our experience with the calibration of the response factors and from the normalizing action of the integrator we may estimate the uncertainty in the phase compositions to be $\delta x = 0.004x_1x_2$ in the mole fraction, with the minimum detectable amount being 0.0002.

Results

Data for the system carbon dioxide + isobutane were measured on four isotherms, 310.93 (100 °F), 344.26 (160 °F), 369.26 (205 °F), and 394.26 K (250 °F). The results are given in Table II and displayed in Figure 2. For the system CO₂ + *n*-butane data were measured on the same isotherms with the exception of the first isotherm, which was measured before the temperature control was perfected. As a result these data were measured at a different temperature, 309.1 K, and they are less accurate and less precise. They are included here because of the existence of several other sets of data at approximately the same temperature. When allowances are made for temperature differences, these data agree quite well with the results of Besserer and Robinson (2) and of Olds et al. (5). Results for the system carbon dioxide + *n*-butane are given in Table III and Figure 3.

In Figure 2 three of the isotherms can be compared directly with the data of Besserer and Robinson (7). Much of the data

Table II. Experimental Results for the CO₂ + *i*-C₄H₁₀ System (Component 1, CO₂)

<i>P</i> /bar	<i>x</i> ₁ /%	<i>y</i> ₁ /%	<i>P</i> /bar	<i>x</i> ₁ /%	<i>y</i> ₁ /%
<i>T</i> = 310.93 K					
4.97	0	0	44.56	53.8	86.01
5.73	0.95	11.5	47.53	58.2	86.87
7.79	3.49	33.0	50.37	62.4	87.6
9.54	5.67	44.40	52.50	65.3	88.16
12.07	8.87	54.96	54.97	68.9	88.73
16.76	14.79	66.61	58.19	73.4	89.52
21.54	21.32	73.29	60.38	76.4	90.2
25.84	27.15	77.38	64.07	80.95	91.0
29.59	32.2	79.93	68.29	85.9	91.8
33.65	38.0	82.2	70.42	88.23	92.2
38.34	44.70	84.03	72.05	90.04	92.3
41.62	49.62	85.11			
<i>T</i> = 344.26 K					
11.15	0	0	49.58	36.35	69.04
12.07	0.84	7.2	53.23	39.93	70.16
13.36	2.10	14.1	57.14	43.73	71.10
14.90	3.50	21.6	61.06	47.44	71.93
16.47	5.00	27.74	64.84	51.10	72.32
18.95	7.38	35.81	68.44	55.39	72.36
24.33	12.42	47.8	71.96	59.74	71.68
31.82	19.31	57.6	73.04	61.18	70.76
36.70	24.09	62.2	73.50	62.35	69.6
40.35	27.55	64.49	74.00	63.32	69.1
44.35	31.55	66.60			
<i>T</i> = 369.26 K					
18.48	0	0	46.56	23.23	48.2
21.55	2.50	10.5	50.23	26.40	49.54
24.52	5.0	19.3	54.32	30.1	51.30
29.37	8.95	29.05	59.85	35.0	52.67
33.85	12.66	35.75	62.11	37.3	52.27
35.53	14.07	38.3	63.76	39.4	52.05
38.36	16.40	41.1	65.58	42.6	50.4
42.62	20.0	45.0	66.09	43.1	50.4
<i>T</i> = 394.26 K					
28.93	0	0	47.20	15.53	22.5
31.42	1.95	4.82	48.72	17.13	22.1
33.69	3.77	8.8	49.09	17.62	23.27
37.67	6.93	14.3	48.98	17.59	22.68
41.09	9.85	18.15			

agree fairly well. However, at the lowest temperature there is some disagreement on the dew curve and near the critical point. At the highest temperature the dew curves differ by several mole percent. In addition in Table I the vapor pressures of isobutane from ref 7 are seen to be much too high, indicating the possible presence of a volatile impurity. In Figure 3 our results are compared with those of Olds, Reamer, Sage and Lacey (5), and we see that the agreement is good with only a few data on the dew curve differing by ≈ 1 mol % near the critical point. The same isotherm was also measured by Hsu, Nagarajan and Robinson (6), and comparison indicates agreement with the present data within about 0.3–0.4 mol %. The data of Leu and Robinson (8) seem to agree quite well with our results when adjustments are made for the small temperature differences between the two sets. We noted, however, that their vapor pressures for pure isobutane appear to be too high, consistent with their earlier results in ref 7. The data for both systems in the near-critical region have been correlated with the Leung-Griffiths model modified by Rainwater and Moldover (14).

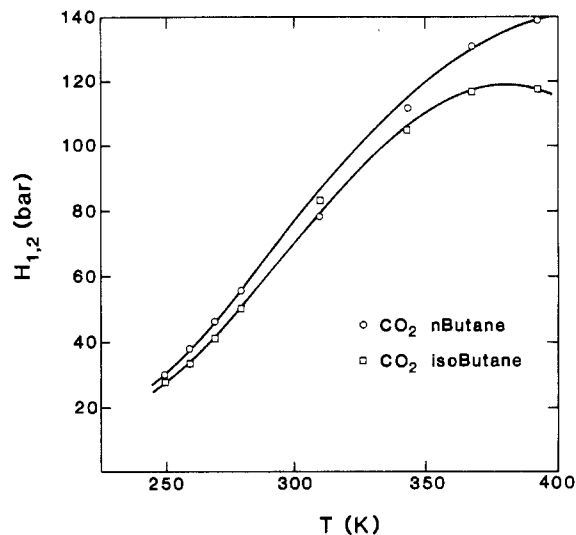
The precision of the dilute solution data made possible the calculation of Henry's constant for carbon dioxide dissolved in the butanes. For this purpose the relationship

$$H_{1,2} = \hat{\phi}_1^\infty [P_2^\sigma + \Delta Z_2(dP/dx_1)^\infty] \quad (1)$$

was used (15). Here $\hat{\phi}_1$ is the fugacity coefficient in the vapor phase of CO₂ in solution, P_2^σ is the vapor pressure of the butane, and ΔZ_2 is the difference between the compressibility

Table III. Experimental Results for the CO₂ + *n*-C₄H₁₀ System (Component 1, CO₂)

<i>P</i> /bar	<i>x</i> ₁ /%	<i>y</i> ₁ /%	<i>P</i> /bar	<i>x</i> ₁ /%	<i>y</i> ₁ /%
<i>T</i> = 309.1 K					
3.36	0	0	37.93	45.0	87.9
4.41	0.68	10.9	48.63	61.9	89.9
6.82	2.4	27.	55.59	72.9	91.8
10.02	4.7	48.4	64.85	85.5	93.6
10.59	8.5	61.6	30.84	34.9	84.9
24.57	26.2	81.3			
<i>T</i> = 344.26 K					
8.32	0	0	27.40	16.6	62.9
9.33	0.91	8.42	31.07	19.8	66.3
12.77	3.91	29.8	40.56	28.2	72.1
13.42	4.46	34.0	47.93	35.1	75.8
16.38	6.99	43.7	57.92	44.3	78.0
17.90	8.22	47.7	62.30	48.3	78.4
20.80	10.83	53.67	67.53	53.5	79.1
25.83	15.2	61.2	72.92	59.0	79.2
<i>T</i> = 369.26 K					
14.17	0	0	59.31	34.15	63.4
16.06	1.36	9.2	67.27	40.7	65.2
18.87	3.46	19.7	75.01	47.9	64.3
25.16	8.10	36.3	78.54	52.6	62.9
38.8	18.55	53.4	79.51	55.3	59.3
40.52	19.76	56.4	78.95	53.3	60.4
48.33	25.7	59.8	78.54	52.6	60.9
57.19	32.5	62.9			
<i>T</i> = 394.26 K					
22.52	0	0	60.45	27.60	44.2
30.30	5.31	18.4	65.02	32.72	39.44
34.57	8.24	25.0	64.87	32.64	39.87
42.47	13.72	33.94	63.83	30.82	41.48
47.70	17.45	38.2	62.34	29.22	42.82
51.93	20.62	41.1	58.06	25.24	42.92
55.44	23.27	42.5	65.55	34.97	38.8

**Figure 4.** Henry's constant for CO₂ dissolved in *n*-butane and iso-butane.

factors of vapor and liquid butane at its vapor pressure. The superscript ∞ refers to the infinitely dilute solution. The ϕ 's and Z 's were calculated from an extended corresponding states model which uses a reference fluid equation of state and a conformal solution principle (16). The resulting Henry's constants at the corresponding butane vapor pressures are given in Table IV and in Figure 4. Also given are the values derived from the data in ref 7 at 250–280 K. The two curves are very similar except at the highest temperature where we see an apparent maximum for the system with iso-butane. This situation is due to the proximity of the critical point of iso-butane, at which point it becomes a much better solvent.

Table IV. Henry's Constants for Carbon Dioxide Dissolved in the Butanes^a

<i>T</i>	<i>H</i> _{1,2}	<i>T</i>	<i>H</i> _{1,2}
CO ₂ + Isobutane			
250.00	27.6	310.93	82.9
260.00	33.4	344.26	105.2
270.00	41.1	369.26	116.3
280.00	50.5	394.26	117.3
CO ₂ + <i>n</i> -Butane			
250.00	29.8	309.1	78.3
260.00	37.7	344.26	111.5
270.00	45.9	369.26	130.7
280.00	55.5	394.26	138.7

^a *T* in K and *H*_{1,2} in bar.

Table V. Estimates for the Values of the Parameters in Equation 2

<i>T</i>	<i>A</i>	<i>B</i>	<i>T</i>	<i>A</i>	<i>B</i>
CO ₂ + Isobutane					
250.00	0.998	0.354	310.93	0.851	0.309
260.00	0.911	0.333	344.26	1.140	0.371
270.00	0.850	0.291	369.26	1.398	0.370
280.00	0.791	0.240	394.26	2.08	0.42
CO ₂ + <i>n</i> -Butane					
250.00	1.115	0.397	309.1	1.000	0.341
260.00	1.020	0.328	344.26	1.199	0.383
270.00	0.968	0.297	369.26	1.469	0.398
280.00	0.921	0.264	394.26	2.13	0.58

We have also estimated values for the excess Gibbs free energy of the saturated liquid, which is adequately described by the two-parameter Redlich-Kister expansion

$$G^E/RT = x_1 x_2 [A + B(x_1 - x_2)] \quad (2)$$

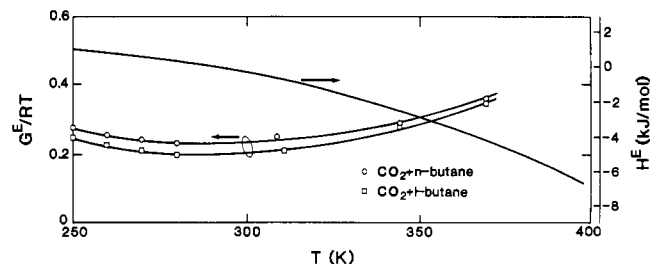
This was done by calculating the fugacity of the mixture *f* for each datum by means of the relationship

$$\ln f = x_1 \ln(\hat{f}_1/x_1) + x_2 \ln(\hat{f}_2/x_2) \quad (3)$$

where $\hat{f}_i = \hat{\phi}_i y_i P$, using the experimental *x*, *y*, and *P*, and $\hat{\phi}$ calculated from ref 16. Each isotherm was then fit with the relationship

$$\ln f = x_1 \ln f_1 + x_2 \ln f_2 + G^E/RT + \int_P^{P_2^s} (V^s/RT) dP \quad (4)$$

where *V*^s is the molar volume of the mixture and *f*₁ and *f*₂ are the fugacities of the pure component liquids. Here *f*₁ corresponds to a hypothetical liquid CO₂ above its critical point, and it was used merely as an adjustable parameter. The integral adjusts the data to a constant pressure, the vapor pressure of the butane. In this equation *G*^E is the excess Gibbs function in the symmetric convention, represented by eq 2. The equation has four adjustable parameters, linear combinations of which allow us to calculate *A* and *B* in eq 2 and also an independent value for Henry's constant *H*_{1,2}. Equation 4 can be applied to data both below and above the critical temperature of the more volatile component. However, as *T* approaches the critical point of the solvent, the extrapolation from the solubility limit to the pure solute fugacity, *f*₁, becomes very long, and the resulting parameters in the equation become less reliable. Nevertheless, the equation was applied to all of the data. The results, given in Table V, look reasonable even though the highest experimental temperature, 394.26 K, approaches the critical temperatures of isobutane and *n*-butane (408.0 and 425.2 K, respectively). The resulting *G*^E/*RT* for equimolar mixtures is shown in Figure 5, where we see that the two curves are very similar. Representing *G*^E with a simple function

**Figure 5.** Estimated excess Gibbs function and excess enthalpy for equimolar mixtures of CO₂ with the butanes. See text.

allows us to calculate the excess enthalpy *H*^E via the relationship

$$H^E/RT^2 = -[\partial(G^E/RT)/\partial T]_{P,x} \quad (5)$$

Although *P* is not strictly constant, the correction is expected to be small. The resulting estimates for *H*^E are also plotted in Figure 5. The values of *H*^E are the same for both systems within the uncertainty and thus are given by a single curve. The excess enthalpy is here identified with the heat of mixing for a process in which pure liquid butane is combined with (hypothetical) liquid CO₂ at constant *T* and *P* to produce a liquid solution. From the curves we see that this heat of mixing changes sign near room temperature. The Henry's constants resulting from eq 5 agree with the ones given in Table IV within a few percent.

Conclusions

We have given a description of a new apparatus for vapor-liquid equilibrium measurements in the 300–500 K range. Data for the binary systems of carbon dioxide with *n*-butane and isobutane are presented and compared with existing data in the literature where they coincide. In general the agreement is good although several discrepancies are noted. Excess Gibbs functions and excess enthalpies are estimated.

Registry No. CO₂, 124-38-9; *n*-butane, 106-97-8; isobutane, 75-28-5.

Literature Cited

- Weber, L. A. *Cryogenics* **1985**, *25*, 338.
- Besserer, G. J.; Robinson, D. B. *Can. J. Chem. Eng.* **1971**, *49*, 651.
- Behrens, P. K.; Sandler, S. I. University of Delaware, private communication.
- Poettmann, F. H.; Katz, D. L. *Ind. Eng. Chem.* **1945**, *37*, 847.
- Olds, R. H.; Reamer, H. H.; Sage, B. H.; Lacey, W. N. *Ind. Eng. Chem.* **1949**, *41*, 475.
- Hsu, J. J.-C.; Nagarajan, N.; Robinson, R. L. *J. Chem. Eng. Data* **1985**, *30*, 485.
- Besserer, G. J.; Robinson, D. B. *J. Chem. Eng. Data* **1973**, *18*, 298.
- Leu, A. D.; Robinson, D. B. *J. Chem. Eng. Data* **1987**, *32*, 444.
- Haynes, W. M.; Goodwin, R. D. *Natl. Bur. Stand. (U.S.) Monogr.* **169**, 1982.
- Goodwin, R. D.; Haynes, W. M. *Natl. Bur. Stand. (U.S.) Tech. Note* **1051**, 1982.
- Levelt Sengers, J. M. H.; Chen, W. T. *J. Chem. Phys.* **1972**, *56*, 595.
- Fernandez-Fassnacht, E.; del Rio, F. *Cryogenics* **1985**, *25*, 204.
- Oguchi, K.; Tanishita, I.; Watanabe, K.; Yamaguchi, T.; Sasayama, A. *Bull. Jpn. Soc. Mech. Eng.* **1975**, *18*, 1456.
- Rainwater, J. C.; Moldover, M. R. in *Chemical Engineering at Supercritical Fluid Conditions*; Paulaitis, M. E., et al., Eds.; Ann Arbor Science Publications: Ann Arbor, MI, 1983; p 199.
- Van Ness, H. C.; Abbott, J. M. *Classical Thermodynamics of Non Electrolyte Solutions*; McGraw Hill: New York, 1982.
- Ely, J. F. National Institute of Standards and Technology (formerly NBS), Boulder, CO, private communication.

Received for review March 29, 1988. Accepted October 19, 1988. Apparatus development was supported by the U.S. Department of Energy, Division of Engineering and Geosciences, Office of Basic Energy Sciences. The experimental work was supported by the Supercritical Fluid Properties Consortium at the National Bureau of Standards, Boulder, CO. Members of the consortium are Air Products and Chemicals, Inc., Allied-Signal Corporation, Amoco Production Company, ARCO Transportation Co., Cooper-Bessemer Reciprocating, E. I. du Pont de Nemours and Co., Gas Processors Association, Mobil Research and Development Corp., Monsanto Company, Phillips Petroleum Co., Shell Development Co., SOHIO, Ingersoll-Rand Co., and Texaco, Inc.